

## Article

# Spatial Analysis of Heavy Metal Pollution in Road-Deposited Sediments Based on the Traffic Intensity of a Megacity

Angélica Vanessa Goya-Heredia <sup>1,2</sup>, Carlos Alfonso Zafra-Mejía <sup>1,3,\*</sup>  and Hugo Alexander Rondón-Quintana <sup>3</sup> 

<sup>1</sup> Maestría en Desarrollo Sustentable y Gestión Ambiental, Facultad del Medio Ambiente y Recursos Naturales, Universidad Distrital Francisco José de Caldas, Carrera 5 Este 15–82, Bogotá E-111711, Colombia; angelica.goya@udc.es

<sup>2</sup> Grupo de Ingeniería del Agua y del Medio Ambiente—GEAMA, Centro de Innovación Tecnológica en Edificación e Enseñaría Civil—CITEEC, Universidade da Coruña, Campus de Elviña s/n, E-15008 A Coruña, Spain

<sup>3</sup> Grupo de Investigación en Ingeniería Ambiental—GIIAUD, Facultad del Medio Ambiente y Recursos Naturales, Universidad Distrital Francisco José de Caldas, Carrera 5 Este 15–82, Bogotá E-111711, Colombia; harondonq@udistrital.edu.co

\* Correspondence: czafra@udistrital.edu.co; Tel.: +57-601-323-9300 (ext. 4040)

**Abstract:** Population growth has led to the intensification of average daily traffic (ADT), highlighting vehicles as one of the major sources of heavy metal (HM) pollution in cities. The objective of this paper is to conduct a spatial analysis of the HM pollution associated with road-deposited sediments (RDSs), based on the ADT observed in the main roads of a Latin American megacity (Bogotá, Colombia). The following risk indices were considered: Geoaccumulation Index (Igeo), Integrated Pollution Index (IPI), Ecological Risk Index (ERI), Comprehensive Potential Ecological Risk Index (CERI), Hazard Index (HI), and Carcinogenic Risk Index (CRI). The findings confirm that a size fraction < 250 µm is the most suitable for studying the risk of HMs in the RDS from the indices considered. The best HMs indicative of the relationship with ADT are Ni, Cu, and Pb. The Pb is the HM of most attention, and Cr gains positions for its toxicity level during the evaluation of ecological, non-carcinogenic, and carcinogenic risks, respectively. Finally, the linear regression models developed between ADT and each of the risk indices considered have a better fit ( $R^2 > 0.910$ ) compared to the linear regression models developed between ADT and HM concentrations ( $R^2 > 0.322$ ).

**Keywords:** heavy metal; megacity; road-deposited sediment; traffic intensity; urban pollution



**Citation:** Goya-Heredia, A.V.; Zafra-Mejía, C.A.; Rondón-Quintana, H.A. Spatial Analysis of Heavy Metal Pollution in Road-Deposited Sediments Based on the Traffic Intensity of a Megacity. *Atmosphere* **2023**, *14*, 1033. <https://doi.org/10.3390/atmos14061033>

Academic Editor:  
Alexandra Monteiro

Received: 15 May 2023  
Revised: 7 June 2023  
Accepted: 8 June 2023  
Published: 15 June 2023



**Copyright:** © 2023 by the authors. Licensee MDPI, Basel, Switzerland. This article is an open access article distributed under the terms and conditions of the Creative Commons Attribution (CC BY) license (<https://creativecommons.org/licenses/by/4.0/>).

## 1. Introduction

In urban areas, there was a direct association between population growth and the increase in road surfaces and number of vehicles. This population growth led to the intensification of average daily traffic (ADT), highlighting vehicles as one of the largest pollution sources (water, air, and soil) in cities. This was also evidenced by the report of a significant relationship between ADT and concentrations of various pollutants present in road environments [1,2]. Urban pollutants were constantly emitted and transported within air masses and tended to accumulate in road-deposited sediment (RDS) [3]. The RDS originated from the accumulation of particles from natural (e.g., soil drag) and anthropogenic sources (e.g., vehicular traffic, industries, and construction), which generated a heterogeneous and complex mixture of pollutants due to their various emission sources [4–6]. Thus, RDSs acted as a sink for hazardous substances for both public health and the environment [7]. These RDSs were able to reach surrounding environments and water bodies through processes such as wind- and traffic-induced resuspension and surface runoff washing [8,9].

Studies have reported that urban RDSs are associated with high heavy metal (HM) concentrations compared to those observed in urban and agricultural soils [10,11]. There are studies that reported Pb, Cu, Zn, Cd, Cr, and Ni as those HMs of greatest interest in

RDSs. This is due to their harmful effects, accumulation characteristics in the human body, and environmental effects on water systems, soil, and air [12–14]. Thus, RDSs have become a possible pollution indicator by HMs in urban environments [15].

In the HM analysis associated with RDSs, the activities developed at the study site from land use, the means of transport involved, and the physical and chemical characteristics of the sediment particles and metallic elements of interest were often considered [16]. Urban studies were also carried out in which the possible relationship between ADT- and RDS-associated MH concentration was reported (e.g., [17,18]). This was under the hypothesis that ADT was possibly one of the main influential variables of the HM concentration associated with urban RDSs [19]. Historically, the first HM reported in this context was Pb for its use as an additive in gasoline. Over the years, the ban on Pb in gasoline limited its use as a possible indicator of ADT. Although, due to its bioavailability, this HM remains of great importance in studies on RDS [20,21]. As more studies are conducted, other HMs (e.g., Cu and Zn) have been identified as possible indicators of the relationship between their concentrations in the RDS and ADT [22,23].

As visualized, in the RDS collected in high traffic roads, there was a high HM content [24]. This is probably due to the growing demand for new high-performance materials for the automotive industry, which has generated a wide variety of components such as steel, fiberglass, and plastic. Indeed, these materials are known for their high HM content [25,26]. High-performance materials are frequently used in tires and brakes, which due to their particular characteristics of use and wear (emission source), makes it difficult to understand the behavior of HM concentrations in urban RDSs. Several studies have sought to relate the origin of HMs in the RDS with the different parts of vehicles and elements of highways and roads (e.g., type of pavement and road furniture), where the operation of these systems plays an important role [27,28]. Moreover, studies have been conducted on the spatiotemporal variation in the HM concentration in RDSs, where it was identified that the highest concentrations were associated with the finest particles and the main vehicular sources were fuel and lubricating oil leaks, brake and tire wear, and combustion gases [29]. It has also been reported that vehicular traffic may have contributed more than 50% of the pollution in RDSs [30].

In recent years, an important variety of studies has been carried out worldwide using evaluation indices of geochemical background concentrations (e.g., Geoaccumulation Index—Igeo and Integrated Pollution Index—IPI) (e.g., [31,32]). These studies have been fundamental to adapt those indices to the integral analysis of HMs in the RDS, through criteria such as the level of toxicity, persistence in the environment, and biological accumulation. This has also allowed an ecological and public health risk assessment to take place due to HMs associated with the RDS, with ecological risk, and non-carcinogenic and carcinogenic risk indices [27,33]. In different studies, there were also joint evaluations between indices. For example, Ecological Risk Index—ERI and contamination factor—CF indices have been used to assess the risk to the biological community from exposure to HMs associated with RDSs [34]. In addition, indices used for assessing human health risk (e.g., Hazard Index—HI and Cancer Risk Index—CRI) have allowed the study of exposure to the HMs associated with the RDS to take place through the following three pathways: Ingestion—HI<sub>ing</sub>, inhalation—HI<sub>inh</sub>, and dermal—HI<sub>der</sub> [35,36]. This has made it possible to study both carcinogenic and non-carcinogenic risks by classifying the community by age groups and exposure time [37]. It was also identified that the ingestion of RDS particles was possibly the main route of exposure to HMs for the elderly and children due to the amounts ingested and their low body weight [38,39].

The objective of this paper is to show a spatial analysis of the HM pollution associated with RDSs from the ADT observed in the main roads of a Latin American megacity (Bogotá, Colombia). We developed regression models between HM concentrations and ADT from local and international reference information. The key aspects of the risk indices considered for the spatial analysis of HM pollution are as follows: metal enrichment, environmental risk, and risk to human health. In addition, we developed regression models between ADT

and the risk indices considered. We also performed a comparative analysis between ADT, HM concentrations, and the limit values established by international reference guidelines. In the context of urban HM pollution, this study is relevant for the following aspects. (1) To evaluate the usefulness of ADT as an indicator variable of the spatial variation in HM concentrations in the RDS. (2) To enhance knowledge regarding the spatial variation in HM concentrations in RDSs of megacities with high ADTs. (3) Analyze existing ecological and human health risks from HM concentrations associated with RDSs of a high-altitude Latin America megacity. (4) To argue that the use of risk indices to assess HM pollution levels is a useful approach that can help policy makers and urban planners develop effective strategies to reduce pollution levels.

## 2. Materials and Methods

### 2.1. Study Site

This study was conducted in the high-altitude megacity of Bogotá, Colombia, South America (2600 m.a.s.l.; 4°35'57" N–74°04'51" W; see Figure 1). The population of the megacity was approximately 9 million inhabitants, which increased to more than 10 million inhabitants with the inclusion of its metropolitan area (5235 km<sup>2</sup>) [40]. The city of Bogotá is the main economic, industrial, cultural, and political center of Colombia. The urban area of the city is approximately 478 km<sup>2</sup> and it has a high population density (17,700 inhabitants/km<sup>2</sup>) [41]. Bogotá is located near the equator. Thus, the climate of the megacity is tropical mountain with a significant hourly temperature variation (7–19 °C) [42]. On average, the annual climate characteristics of the megacity during the study period were as follows: rainfall = 1050 mm, temperature = 13 °C, wind speed = 9.6 km/h, and relative humidity = 75%. The megacity had a high motorization rate during the study period (313 vehicles/1000 inhabitants). The vehicle fleet during the study period was 2.5 million vehicles, distributed as follows: passenger cars = 46%, pickup truck = 25%, motorcycles = 22%, heavy trucks = 3%, taxis = 2%, and public transport buses = 2% [43]. Private vehicles and motorcycles use mainly gasoline, taxis use natural gas and gasoline, buses use natural gas and diesel, and heavy vehicles use mainly diesel [44]. During the study period, there was a restriction on the circulation of vehicles in the megacity as a measure to reduce traffic congestion. This vehicular restriction prevented about 40% of the passenger cars of the megacity from circulating (between 6 and 9 a.m. and 3 and 7 p.m.) [45].

### 2.2. Calculation of ADT

We developed this study in the main roads of the Latin American megacity of Bogotá (Colombia). We collected ADT information from the installation of 101 automatic traffic-monitoring stations (vehicles/day) distributed throughout the megacity (Figure 1). The District Secretariat of Mobility of the megacity under study administered this information (<https://datos-abiertos-sdm-movilidadbogota.hub.arcgis.com/>, accessed on 30 January 2019) [46]. In addition, we installed eight ADT monitoring stations at the access tolls to the megacity. The National Institute of Roads of Colombia administered this information (<https://www.invias.gov.co/index.php/archivo-y-documentos/documentos-tecnicos/6609-serie-historica-de-transito-promedio-diario-actualizada-tpd-2016-publicacion>, accessed on 30 January 2019) [47]. We also monitored ADT at the nine study sites established to monitor HM concentrations. The ADT referred to the average daily number of vehicles that traveled on each of the 118 selected roads during the period from 2010 to 2018. We collected hourly ADT information (Monday to Friday) and then added it under a daily time scale. We calculated the average daily ADT for each of the selected roads during the study period. This significant number of monitoring stations obtained the adequate density and spatial coverage when making use of geostatistical analysis methods [48]. In this study, we used 118 ADT monitoring stations.

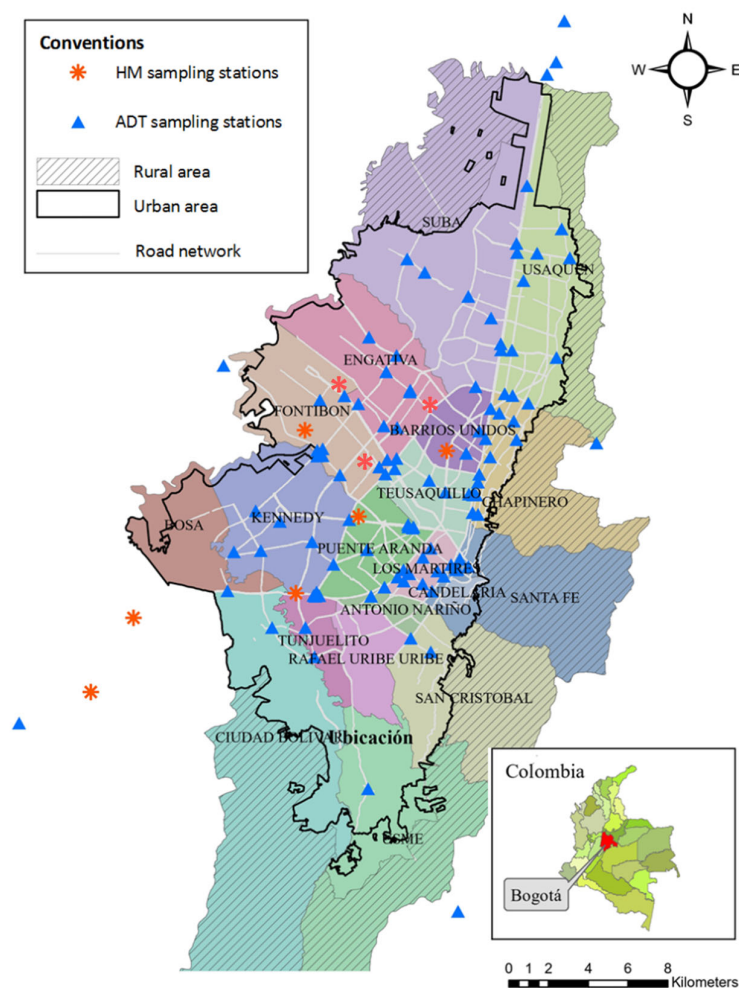


**Figure 1.** Location of ADT and HM monitoring stations in the megacity under study.

### 2.3. Calculation of HM Concentrations

The RDS of nine roads was collected to determine the associated HM concentration (Pb, Zn, Cu, and Cd). The varied characteristics of ADT (570–13,500 vehicles/day) and land use (residential, industrial, and commercial) supported the selection of these nine roads. We collected RDS samples in dry weather at the side of the curb (0.50 m) at the same time over a period of one year. On average, the sampling frequency was 10 days. However, there were slight variations due to the occurrence of rainfall events that prevented the collection of RDS dry. The sampling area had an area of 0.49 m<sup>2</sup> (0.70 m × 0.70 m). We ensured the dimensions of the collection area by placing a wooden frame with identical dimensions to those of the sampling area on the surface. Moreover, we controlled the sampling site to avoid repetition and to be close to previous RDS collection points. For the RDS collection, we used a brush made of plastic fibers and a hand dustpan. Thirty-six samples were collected for each study road (total samples = 324). The protocol for the RDS collection was established, taking as reference the sampling systems reported by other studies on this matter [49–51].

The HM concentration in RDSs was taken for a size fraction < 250 µm. This is because studies have reported that this size fraction tended to show the highest HM concentrations. The researchers attributed this behavior to a larger specific surface area and therefore to a higher adsorption capacity of pollutants [52,53]. Lastly, the HM concentration associated with RDSs was determined by means of inductively coupled plasma equipment (ISO-11047) [54]. RDS samples were previously digested in a mixture of hydrochloric acid and nitric acid (3:1; aqua regia, ISO-11466 method) [55]. The following HMs were analyzed: Pb, Zn, Cu, and Cd.

#### 2.4. Information Analysis

In this study, we conducted a worldwide literature review restricting the search to the period between 1980 and 2018. This literature review considered the total content of documents included in the following scientific databases: Google Scholar, Springer, and ScienceDirect. The keywords used in the search engines were as follows: heavy metals, road sediment, and traffic intensity. We conducted this literature review to generate a database that correlated the HM concentration in the RDS and ADT based on reference studies worldwide and the HM concentrations observed directly in nine roads of the study megacity. The variables considered in this database were as follows: ADT, particle size fraction, and HM concentration. The MHs considered in this literature review were as follows: Pb, Zn, Cu, Cd, Cr, and Ni. The RDS size fraction was considered representative of the HM concentration, which was  $<250 \mu\text{m}$  [56].

The Shapiro–Wilk normality test ( $p$ -value  $< 0.050$ ) [57] was applied to the data series of each variable. Thus, Spearman's correlation coefficient ( $r_s$ ) was used to study the degree of association between the variables considered [50]. For significant correlations, we proceeded to develop linear regression models [58] between ADT and the HM concentration in the RDS (Pb, Zn, Cu, Cd, Cr, and Ni). Descriptive statistics were also used during the information analysis [59]. All previous statistical analyses were executed using the free software R V.3.5.3 [60]. Subsequently, with the linear regression models, we foretold HM concentrations in the RDS using the ADT observed in each of the 118 monitoring stations established throughout the megacity. We used the HM concentrations measured directly on the nine roads of the megacity to validate the forecasts made with the linear regression models previously developed. From the foretold HM concentrations, RDS pollution concentrations in the study megacity were determined and interpreted.

In this study, we used the following risk assessment indices for HM concentrations in the RDS. (1) Metal enrichment: Indices used to assess the influence of anthropic activities on the HM concentration in the RDS from geochemical background concentrations [15]. Thus, the Geoaccumulation Index—Igeo and Integrated Pollution Index—IPI [49] were used. (2) Environmental risk: Indices that allowed an association to be made between ecological and environmental effects with the HM toxicity based on guide concentrations for soil quality. The Ecological Risk Index—ERI and Comprehensive Potential Ecological Risk Index—CERI were then used [61]. (3) Risk to human health: Indices that allowed an analysis of the risks to human health to take place through the three main pathways of exposure (ingestion, dermal contact, and inhalation) and by age group (children and elderly). The Hazard Index—HI (non-carcinogenic), for each metal and for the set of HMs, and the Carcinogenic Risk Index—CRI [59] were used. Table 1 shows all the calculation equations and valuation categories for the indices considered.

Additionally, we applied the inverse distance weighted (IDW) interpolation method using ArcGIS V.10.2. Software [62] to analyze the spatial variation in the HM concentrations (Pb, Cu, Cr, and Ni) and the risk indices considered. The choice of the IDW method was made because it tended to spatially maintain local maximums (unsmoothed) compared to other methods (e.g., Kriging) [63]. This made it possible both to identify the most critical areas (sampling sites) under the context of this study and to estimate the spatial values with respect to the weighting of the sampling roads as a function of their proximity [64]. Namely, we studied the spatial variation in the HM concentrations and indices considered based on the ADT gauging roads. Lastly, the geographical information of the urban area of the megacity was obtained from the IDECA open data portal (<https://www.ideca.gov.co/>, accessed on 1 May 2019) [65].

**Table 1.** Indices considered assessing the risk by HMs present in RDSs.

Type	Index	Equation	Criteria	Valuation	Range
Metal enrichment	Igeo	$I_{geo} = \log_2 \times [C_i / (1.5 \times B_i)]$	$C_i =$ Reference HM concentration [mg/kg]	Unpolluted	$I_{geo} < 0$ $0 < IPI \leq 1$
			$B_i =$ Background concentration for each HM [mg/kg]	Unpolluted–Moderate	$0 < I_{geo} < 1$ $1 < IPI \leq 2$
			1.5 = Correction factor	Moderate	$1 < I_{geo} < 2$ $2 < IPI \leq 3$
	IPI	$IPI = [(Cf_1) \times (Cf_2) \times (Cf_3) \times \dots (Cf_n)]^{1/n}$	$C_{fi} = C_i / B_i$ Concentration of the reference HM for normalization [mg/kg]	Moderate–High	$2 < I_{geo} < 3$ $3 < IPI \leq 4$
			$n =$ Number of HMs considered	High	$3 < I_{geo} < 4$ $4 < IPI \leq 5$
				High–Extremely high	$4 < I_{geo} < 5$ $IPI > 5$
Environmental risk	ERI	$CERI = \sum Er^i$	$CERI =$ Comprehensive potential Ecological Risk Index. $Er^i =$ Potential ecological risk factor for each HM. $Tr^i =$ Toxic factor of HM (Zn = 1, Cr = 2, Pb = Cu = 5, Cd = 30)	Low	$ERI < 40$ $CERI < 150$
				Moderate	$40 \leq ERI < 80$ $150 \leq CERI < 300$
				Considerable	$80 \leq ERI < 160$ $300 \leq CERI < 600$
				High–Very high	$ERI \geq 160$ $CERI \geq 600$
Risk to human health	HI	$HI = HQ_{ing} + HQ_{inh} + HQ_{der}$	HQ = Risk quotient on human health. ADDi = Average daily dose by pathway of exposure [mg/(kg × day)]. RfDi = Reference dose per HM and pathway of exposure [mg/(kg × day)]	Non-significant risk	$HQ \leq 1$ $HI \leq 1$
	HQ	$HQ_{ing} = (ADD_{ing}) / RfD_{ing}$ $HQ_{inh} = (ADD_{inh}) / RfD_{inh}$ $HQ_{der} = (ADD_{der}) / RfD_{der}$		Significant risk	$HQ > 1$ $HI > 1$
	CRI	$CRI = LADD \times SF$		Non-significant risk	$CRI < 1 \times 10^{-4}$

Note. Igeo = Geoaccumulation Index, IPI = Integrated Pollution Index, ERI = Ecological Risk Index, HI = Hazard Index (non-carcinogenic), HQ = non-carcinogenic risk quotient by pathway of exposure, CRI = Carcinogenic Risk Index, HQing = ingestion, HQinh = inhalation, and HQder = dermal contact.

### 3. Results and Discussion

#### 3.1. Worldwide Comparative Analysis

The results of the worldwide literature review showed the following order of importance according to the HM concentration associated with RDSs: Zn > Pb > Cu > Cr > Ni > Cd (Table 2). The HMs analyzed in the study megacity showed the following order of importance from the concentrations detected: Zn > Cu > Pb > Cd. Thus, we observed that both globally and locally, the three HMs with the highest concentration in RDSs were in the following order of importance: Zn, Pb, and Cu. We also evidenced that the average HM concentrations in the megacity under study were within the worldwide range. Moreover, the findings confirmed a size fraction < 250 μm as the most globally representative to study the HM concentration in RDSs (see median in Table 2).

In this study, we performed a Spearman correlation analysis of the worldwide information shown in Table 2 (Figure 2). This is representative of the size fraction of the HM concentration in RDSs (<250 μm). The results showed a significant positive correlation from medium to strong between the size fraction < 250 μm and the concentrations of Cr (rs = 0.681) and Ni (rs = 0.763). In addition, we observed significant positive correlations of weak to medium between the following concentrations of HMs: Zn–Cr (rs = 0.389) and Cd–Ni (rs = 0.417). In order of importance, significant positive correlations from medium to strong were evidenced between the following HMs: Cu–Ni (rs = 0.817), Cr–Ni (rs = 0.810), Pb–Zn (rs = 0.790), Pb–Cd (rs = 0.737), Zn–Cu (rs = 0.723), Pb–Ni (rs = 0.702), Zn–Cd (rs = 0.701), Pb–Cu (rs = 0.644), Zn–Ni (rs = 0.605), Cu–Cd (rs = 0.581), and Cu–Cr (rs = 0.573). The results suggested that for the latter group of HMs (Cu, Ni, Pb, Zn, Cd, and Cr), the pollution source was probably the same. Indeed, in the road environments, the main source reported was vehicular traffic [66]. Other studies (e.g., [5,67]) reported that the main sources of Zn, Pb, and Cd in road environments were associated with wear of engine parts, road demarcation paint, pavement, and road equipment.

**Table 2.** Worldwide and local results for the HM concentration in RDSs according to ADTs.

	Fraction ( $\mu\text{m}$ )	ADT (veh./day)	Concentration (mg/kg)					
			Pb	Zn	Cu	Cd	Cr	Ni
America (12.8%)								
Median	<1000	52,787	93.5	317.3	163	0.10	81.25	40.0
Average	<1200	61,513	108	320	143	0.00	95.0	45.0
Maximum	<2000	130,000	200	414	236	0.50	203	58.7
Minimum	<63	10,000	31.3	183.7	44.7	0.00	12.9	35.0
Asia (30.8%)								
Median	<250	19,851	134	316	170	2.00	127	49.9
Average	<922	39,301	204	573	215	2.13	183	49.4
Maximum	<2000	144,000	589	1585	510	4.00	530	86.0
Minimum	<53	2400	40.0	51.4	24.0	0.30	58.1	20.0
Europe (41.0%)								
Median	<250	15,450	238	310	135	2.00	74.0	27.5
Average	<580	30,855	413	809	194	5.32	96.1	30.6
Maximum	<2000	120,000	2296	4892	771	22.0	232	67.9
Minimum	<10	1800	1.50	80.0	21.5	0.10	13.0	7.50
Africa (7.70%)								
Median	<250	51,480	251	250	123	0.50	123	38.5
Average	<1113	44,120	264	242	106	6.20	122	32.7
Maximum	<2000	68,520	520	343	151	18.0	123	44.4
Minimum	<200	5000	33.6	125	29.0	0.00	119	9.39
Oceania (7.70%)								
Median	<250	24,000	290	370	124	-	19.0	-
Average	<483	19,266	351	564	127	-	19.0	-
Maximum	<1000	25,000	511	1073	184	-	19.0	-
Minimum	<200	8800	251	249	73.0	-	19.0	-
Total documents considered worldwide (n = 39, 100%)								
Median	<250	20,000	200	318	151	2.50	123	35.0
Average	<755	37,157	308	646	1816	4.50	128	40.5
Maximum	<2000	144,000	2296	4892	771	22.0	530	86.0
Minimum	<10	1800	1.50	51.4	21.5	0.00	12.9	7.50
This study, Bogotá/Colombia (n = 9)								
Median	<250	7525	71.5	136	81.0	0.90	-	-
Average	<250	11,817	92.0	168	108	0.90	-	-
Maximum	<250	40,100	217	334	279	1.10	-	-
Minimum	<250	650	48.0	96.0	41.0	0.70	-	-

Note. n = sample size, ADT = average daily traffic, and Veh. = vehicles.

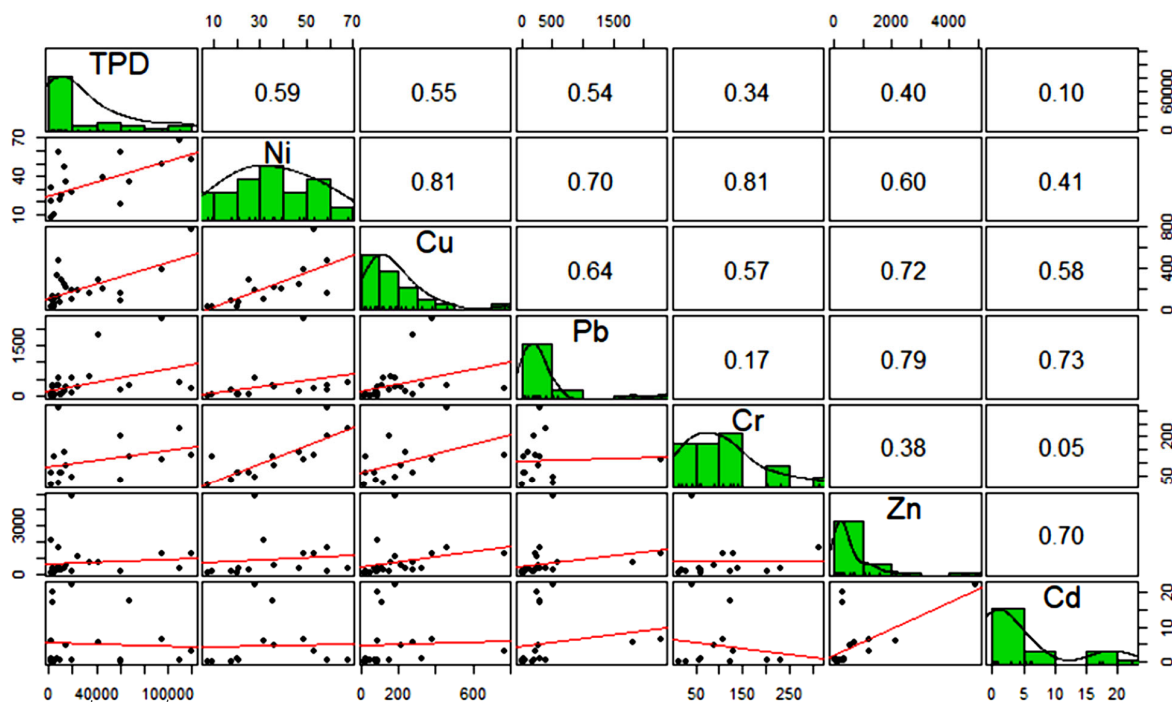


**Figure 2.** Spearman correlation coefficients between HM concentrations (mg/kg) and ADT (veh./day). TPD = average daily traffic.

The findings of the worldwide review showed significant medium to strong positive correlations between ADT and the following HMs: ADT-Ni ( $r_s = 0.598$ ), ADT-Cu ( $r_s = 0.554$ ), and ADT-Pb ( $r_s = 0.543$ ). In addition, we observed significant weak to medium positive correlations between ADT and the following HMs: ADT-Zn ( $r_s = 0.402$ ) and ADT-Cr ( $r_s = 0.340$ ). The results suggested that, in order of importance, the following HMs are the best metallic elements to make the forecasts of HM concentrations in RDSs from the ADT of the megacity under study: Ni, Cu, and Pb. The studies recognized Cu as a key indicator of emissions from wear on vehicle brakes and tires. This shows that these vehicular components contributed significantly to the HM pollution reported in RDSs [27,34]. In addition, there were reports that one of the main sources of Ni in road environments was vehicle exhaust emissions. Emissions from this HM increased by approximately five times because of high exhaust system temperatures during vehicle acceleration. However, it was not ruled out that its pollution source was also likely related to lubricant leaks and wear on parts of the vehicle subjected to chrome plating processes [68,69].

### 3.2. HM Concentration Forecasts

The forecast of the HM concentrations in RDSs of each of the ADT monitoring stations established in the study megacity ( $n = 109$ ) was made based on the correlations calculated between the HM concentrations (size fraction  $< 250 \mu\text{m}$ ) and ADT reported by international reference studies (Figure 2). Different regression models were evaluated, with the linear model providing the best fit between ADT and concentrations of Ni ( $\text{Ni} = 0.0003 \times \text{ADT} + 24.3$ ;  $r_s = 0.598$ ), Cu ( $\text{Cu} = 0.0036 \times \text{ADT} + 99.3$ ;  $r_s = 0.554$ ), and Pb ( $\text{Pb} = 0.0085 \times \text{ADT} + 176.7$ ;  $r_s = 0.543$ ). The results hinted at this group of metallic elements possibly being concentration indicators of other HMs (Zn, Cr, and Cd) from ADT (Figure 2). Namely, from the observed correlations, Zn concentrations in RDSs could be foretold from concentrations of Pb ( $\text{Zn} = 0.569 \times \text{Pb} + 448$ ;  $r_s = 0.797$ ), Cr from Ni ( $\text{Cr} = 3.61 \times \text{Ni} - 9.94$ ;  $r_s = 0.811$ ), and Cd from Pb ( $\text{Cd} = 0.0038 \times \text{Pb} + 1.93$ ;  $r_s = 0.701$ ).

Based on the calculated correlation coefficients ( $r_s$  between 0.543 and 0.811), the results suggested possible errors in the forecasts of HM concentrations from ADT (linear regression models). Thus, we emphasize the importance of having a comprehensive vision in relation

to the behavior of HM concentrations in RDSs. In urban environments, the study of the behavior of HM concentrations in RDSs involved considering other related phenomena such as the surface washing of RDS after rainfall periods, or processes of RDS resuspension by high wind speeds and turbulence generated by vehicular traffic during dry weather [25,70]. From the joint evaluation of these urban dynamics, better adjustments could be obtained in the linear regression models developed for the forecast of HM concentrations in RDSs. The forecasts of the HM concentration ( $n = 109$ ) were validated by the concentrations observed in the study megacity ( $n = 9$ ). The HMs considered for this validation were Pb and Cu. This is because they have been reported to show a significant relationship with ADT (e.g., [68,71]). The results initially showed that foretold concentrations of Pb and Cu tended to be within the worldwide range (Pb: 1.50–2296 mg/kg and Cu: 21.5–1816; Tables 2 and 3). The mean percentage errors of foretold Pb and Cu concentrations in relation to observed concentrations were 8.98% and 10.4%, respectively.

**Table 3.** Observed and foretold Cu and Pb concentrations from ADTs.

Sampling Site	ADT	Observed		Foretold		Error (%)	
		Cu	Pb	Cu	Pb	Cu	Pb
Av. Boyacá-Av. Primero de Mayo	187,600	827	1983	716	1774	6.20	10.5
Av. Suba-CL 100	157,300	712	1692	611	1386	14.1	18.1
Av. Boyacá-Av. Jorge Gaitán Cortés	55,200	324	712	295	639	8.91	10.2
Autopista Norte-CL 200	49,000	300	652	276	593	8.10	9.02
Av. Jorge Gaitán Cortés-Av. Ciudad de Cali	26,900	216	440	191	393	11.6	10.7
KR 24-CL 80	14,200	168	318	150	297	10.4	6.48
KR 13-CL 59	12,500	162	302	144	283	10.9	6.31
CL 45-KR 13	6900	140	248	124	235	11.3	5.11
KR 7-CL 183	4200	130	222	114	212	11.9	4.33

### 3.3. HM Enrichment Risk

In the risk analysis of the metal enrichment of RDSs, we considered the foretold concentrations of the following HMs: Ni, Cu, and Pb. Moreover, Cr concentrations were considered because of their very strong correlation with Ni concentrations ( $r_s = 0.811$ ). The Igeo index was calculated from the background concentrations in urban soils (worldwide average) reported by Alekseenko and Alekseenko [72]. On average, the results showed from the Igeo index that the RDS of the study megacity was not enriched (not polluted) with Ni and Cr ( $I_{geo} < 1$ ). These results were similar to those reported by Li et al. [64] and Wei et al. [73] for the RDS of the Chinese megacities Chengdu and Beijing, respectively. In contrast, the Igeo index for Cu and Pb suggested moderate to high ( $1 < I_{geo} < 4$ ) and moderate to extremely high ( $1 < I_{geo} < 5$ ) metal enrichment in the RDS, respectively. The concentrations of Cu and Pb in RDSs were between 21.5 and 771 mg/kg, and 48 and 217 mg/kg, respectively. Sager et al. [69] also reported high Igeo in RDSs ( $> 3.2$ ) from the cities of Budapest (Hungary) and Seoul (South Korea). The area of highest metal enrichment by these two HMs was located southwest of the study megacity (Figure 3). However, Pb enrichment of the RDS reached to cover a larger percentage area of the megacity (north, center, and south) compared to Cu. This high Pb enrichment of the RDS coincided with the location of the sampling stations with the highest ADT between 2932 and 188,000 veh./day. Lastly, the decreasing order in the Igeo index was as follows: Pb > Cu > Ni > Cr.

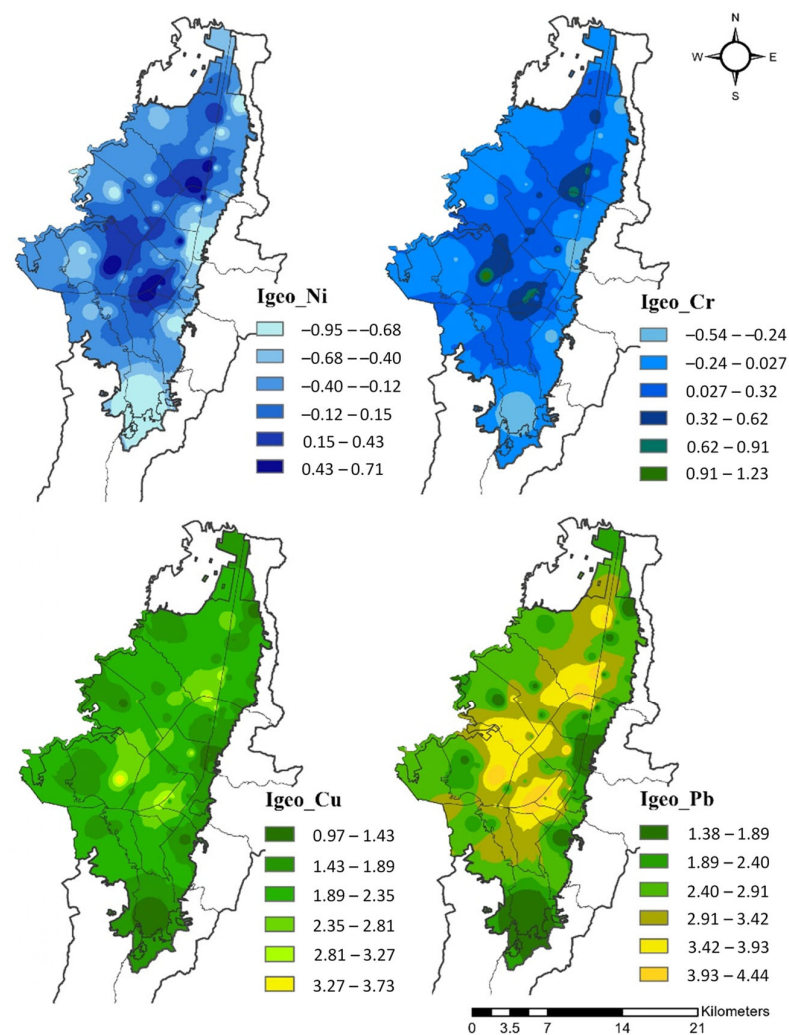


**Figure 3.** Spatial distribution of the Igeo index in the megacity under study (Ni, Cr, Cu, and Pb).

From the calculation of the IPI index, we conducted a comprehensive analysis in the RDS that considered the following HMs together: Ni, Cr, Cu, and Pb. The results showed an IPI index between 1.74 and 8.64 in the RDS. Namely, we evidenced a moderate to extremely high degree of metallic pollution in the RDS. Gope et al. [74] reported that IPI values  $>1$  in the RDS hinted at a deterioration in the environmental quality of road environments. This is possibly because the HM concentrations observed in the RDS were above the limit of the background values for urban soils. On average, an IPI value = 3.36 was observed throughout the study megacity. However, there were specific areas of extreme pollution (IPI: 5.22–7.48). These areas were in the center and south of the megacity (Figure 4). According to the results of the IPI index, areas with an extreme pollution degree in RDSs were associated with monitoring stations with high ADTs (90,000–188,000 veh./day). The above results were consistent with those reported for the cities of Tehran (Iran) and Asansol (India), where average IPI values of 2.5 and 3.7, respectively, were observed [10,74]. It was also suggested that in urban areas, ADT was one of the main indicators of anthropogenic pollution sources in RDSs [75]. Lastly, Cu and Pb were the main influential HMs in the calculation of pollution degree with the IPI index (joint contribution  $> 80\%$ ).

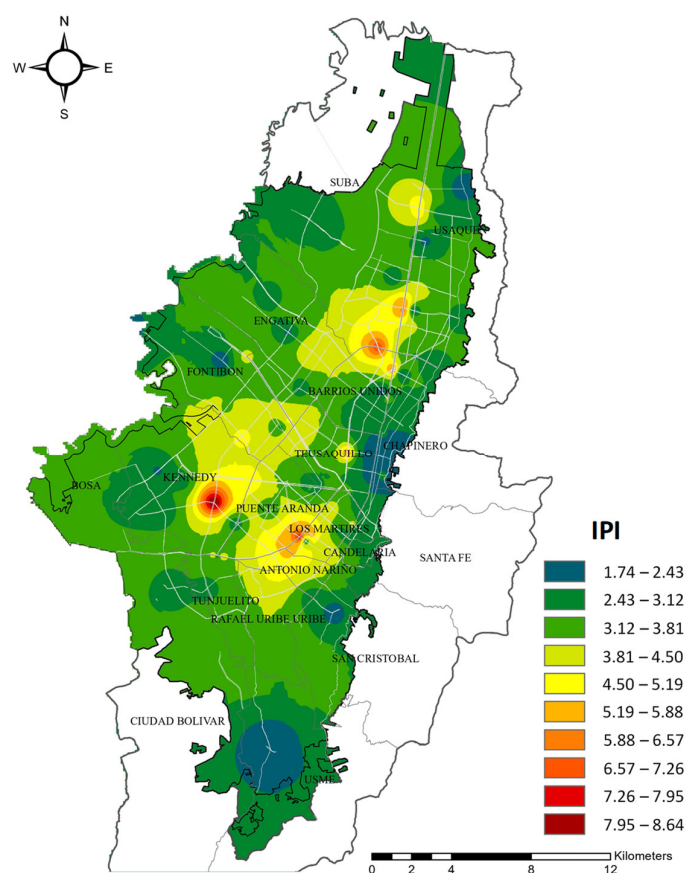


**Figure 4.** Spatial distribution of the IPI index in the megacity under study (Ni, Cr, Cu, and Pb).

In this study, we developed linear regression models between ADT and the Igeo and IPI indices. In other words, we normalized the HM concentrations under the rating scales established by these indices. This normalization meant we could obtain a better fit of the linear regression models between ADT and Igeo and IPI indices ( $R^2 > 0.921$ ) compared to the models developed between ADT and HM concentrations ( $R^2 > 0.322$ ). The linear regression models obtained were as follows:  $I_{\text{geo\_Ni}} = 1 \times 10^{-5} \times \text{ADT} - 0.902$  ( $R^2 = 0.975$ ),  $I_{\text{geo\_Cu}} = 2 \times 10^{-5} \times \text{ADT} + 1.259$  ( $R^2 = 0.935$ ),  $I_{\text{geo\_Pb}} = 2 \times 10^{-5} \times \text{ADT} + 1.763$  ( $R^2 = 0.921$ ),  $I_{\text{geo\_Cr}} = 1 \times 10^{-5} \times \text{ADT} - 0.477$  ( $R^2 = 0.971$ ), and  $\text{IPI} = 4 \times 10^{-5} \times \text{ADT} + 1.615$  ( $R^2 = 0.989$ ).

### 3.4. Environmental Risk

In the analysis of the environmental risk of HMs in RDSs, we considered the foretold concentrations of the following HMs: Ni, Cu, and Pb. Cr concentrations were also considered because of their very strong correlation with Ni concentrations ( $r_s = 0.811$ ). The results showed the following decreasing order in the Ecological Risk Index (ERI) according to each HM:  $\text{Pb} > \text{Cu} > \text{Cr} > \text{Ni}$ . The RDS of the study megacity showed at most an ERI index for Ni, Cr, and Cu of low ( $\text{ERI} < 27$ ), considerable ( $\text{ERI} < 141$ ), and considerable ( $\text{ERI} < 160$ ) risk, respectively (Figure 5). However, there are sectors of the megacity that showed a high ERI for Pb ( $\text{ERI} = 355$ ). These sectors were in the center and south of the megacity. Indeed, we observed Pb concentrations of up to 217 mg/kg in these sectors. These findings hinted at the occurrence of urbanization processes characterized by the increase in unregulated anthropic activities and with high population densities. In the cities of Ezhou (China) and Cairo (Egypt), a similar trend was reported, where Pb, Cu, and Cr were the HMs that showed a higher ERI index, which was possibly due to their high toxicity coefficient [76,77]. This trend suggested a large impact on the environment and harmful effects on living organisms in areas surrounding the study roads. This elevated

ERI for Pb in the RDS coincided with the location of monitoring stations with higher ADTs (83,000–188,000 veh./day).

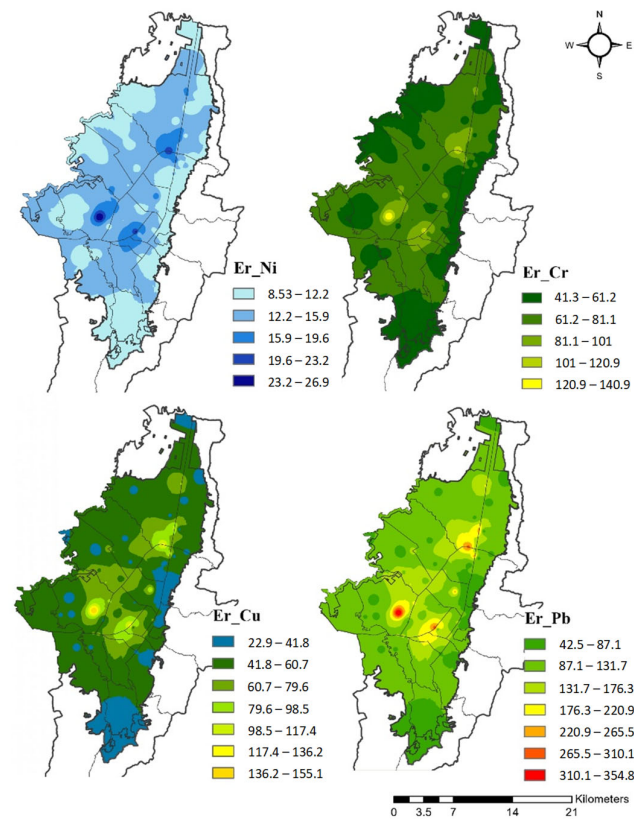


**Figure 5.** Spatial distribution of the ERI (Er) index in the megacity under study (Ni, Cr, Cu, and Pb).

Based on the calculation of the CERi index (Comprehensive Potential Ecological Risk Index), we conducted an ecological analysis for the HMs considered in the RDS (Ni, Cr, Cu, and Pb). The results showed values in the CERi index from 115 to 678 in the RDS of the megacity under study. Namely, low to very high ecological risk from HMs associated with the RDS was evident (Table 1). The results showed that ecological risk was mainly associated with the Pb content in the RDS (average contribution = 45.4%), followed by Cr (27.6%), Cu (21.6%), and Ni (5.52%) content. In urban residential sectors and with high ADT, CERi index values of up to 471 (considerable risk) have been reported [59]. On average, a value of CERi = 243 was observed throughout the study megacity (moderate risk). However, there were specific areas with considerable ecological risk (CERi = 546). These areas were in the center and south of the study megacity (Figure 6). According to the results of the CERi index, these areas with a considerable degree of ecological risk in the RDS were associated with monitoring stations with high ADTs (72,000–188,000 veh./day).

Finally, we developed linear regression models between ADT and the ERI and CERi indices. Namely, we normalized the HM concentrations under the valuation scales established by these indices. This normalization allowed a better fit of the linear regression models to be obtained between ADT and ERI and CERi indices ( $R^2 > 0.910$ ) compared to the models developed between ADT and HM concentrations ( $R^2 > 0.322$ ). The linear regression models developed were as follows:  $ERI_{Ni} = 1 \times 10^{-4} \times ADT - 8.11$  ( $R^2 = 0.982$ ),  $ERI_{Cu} = 7 \times 10^{-4} \times ADT + 19.9$  ( $R^2 = 0.939$ ),  $ERI_{Pb} = 1.7 \times 10^{-3} \times ADT + 35.3$  ( $R^2 = 0.931$ ),  $ERI_{Cr} = 1 \times 10^{-4} \times ADT + 38.9$  ( $R^2 = 0.911$ ), and  $CERi = 3.1 \times 10^{-3} \times ADT + 102.3$  ( $R^2 = 0.983$ ).

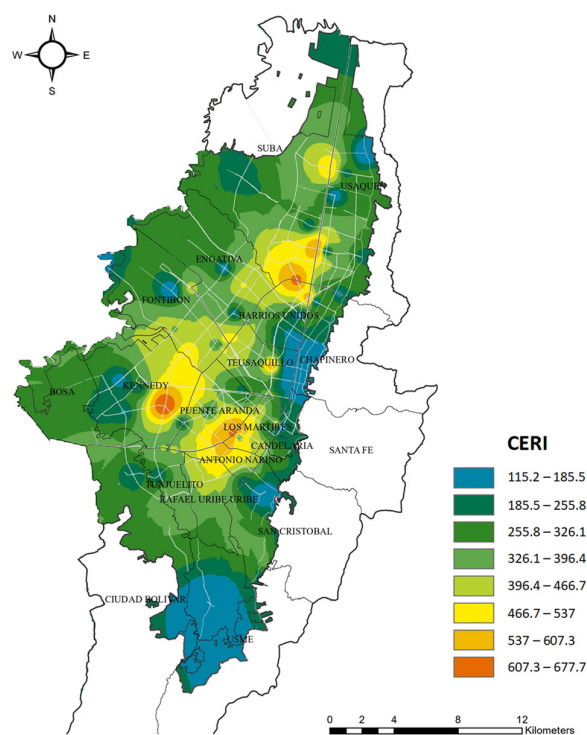


**Figure 6.** Spatial distribution of the CERI index in the megacity under study (Ni, Cr, Cu, and Pb).

### 3.5. Human Health Risk

From the average daily dose of a pollutant, the average HM doses through the following three pathways of exposure were calculated: ingestion, dermal, and inhalation (Table 4). The findings showed that the doses acquired by the population of children were frequently compared to those of the elderly population. This was probably due to the low body weight and high ingestion rates of the child population, which could be prevented through good body hygiene practices [39]. The results showed that Cr and Pb contained in the RDS exceeded the risk quotient on human health considered safe ( $HQ < 1.0$ ) by dermal contact and ingestion in the children population, respectively. However, Cr was in the environment under different physicochemical forms, where Cr (VI) was the most toxic. Previous studies have estimated that, on average, Cr (VI) could be as high as 30% of total Cr [78]. In this study, we considered the maximum value of 30% for Cr (VI) over total Cr for the calculation of the HI-total index (joint evaluation of HMs). Thus, overestimates to which the human health risk assessment for multiple metallic elements (HI-total) could lead to were adjusted. In fact, further studies for the bioavailable fraction of Cr are required to provide accurate results regarding the risks on human health in the study megacity.

The findings revealed specific areas in the study megacity where there was a potential risk to the child population from Pb ingestion associated with the RDS (maximum value of  $HQ_{ing} = 2.28$ ). These areas exceeded the risk limit for ingestion ( $HQ_{ing} > 1.0$ ) and were in the center and south of the megacity (Figure 7). The ADT associated with these study areas was between 77,000 and 180,000 veh./day. Although within the analysis of the elderly population no potential risks were observed for ingestion, dermal contact, and inhalation of RDS with HMs ( $HQ > 1.0$ ), there were study areas with values close to 1.0 for dermal contact with Cr present in the RDS ( $HQ_{der} = 0.904$ ). In the children and elderly populations, risk due to exposure to RDS with Pb had the following order of importance according to the exposure pathway: ingestion > dermal contact > inhalation. In the elderly population, this sequence changed for Cr: dermal contact > ingestion > inhalation. The above findings for the children and elderly populations were consistent with those reported worldwide (e.g., [5,59]). On average, when jointly assessing the risk from exposure to RDS with Pb (ingestion, dermal contact, and inhalation), no non-carcinogenic risk was

observed in the child population (HI = 0.925). However, non-carcinogenic risk was close to the recommended limit value (HI = 1.0). Ingestion, dermal contact, and inhalation of Pb-containing RDSs in the child population contributed a non-carcinogenic risk of 95.9%, 4.09%, and 0.01%, respectively (Table 4). The decreasing order in the HI index for each of the HMs was as follows: Pb > Cr > Cu > Ni.

**Table 4.** Hazard ratio (HQ) and hazard index (HI) for each HM and for the set of HMs (HI-total) in the RDS (children and elderly).

HM	Statistic	HQ Ingestion		HQ Dermal		HQ Inhalation		HI	
		Children	Elderly	Children	Elderly	Children	Elderly	Children	Elderly
Ni	Mean	0.012	0.002	0.017	0.012	$3.32 \times 10^{-13}$	$2.65 \times 10^{-13}$	0.029	0.014
	Median	0.011	0.002	0.015	0.011	$2.98 \times 10^{-13}$	$2.38 \times 10^{-13}$	0.026	0.013
	Max	0.025	0.005	0.035	0.025	$6.92 \times 10^{-13}$	$5.52 \times 10^{-13}$	0.059	0.030
	Min	0.008	0.002	0.011	0.008	$2.17 \times 10^{-13}$	$1.73 \times 10^{-13}$	0.019	0.009
Cr	Mean	0.265	0.052	0.571	0.417	$7.76 \times 10^{-10}$	$8.06 \times 10^{-10}$	0.251	0.141
	Median	0.236	0.047	0.508	0.371	$6.90 \times 10^{-10}$	$7.17 \times 10^{-10}$	0.223	0.125
	Max	0.574	0.113	1.238 *	0.904	$1.68 \times 10^{-9}$	$1.74 \times 10^{-9}$	0.544	0.305
	Min	0.166	0.033	0.359	0.262	$4.87 \times 10^{-10}$	$5.06 \times 10^{-10}$	0.158	0.088
Cu	Mean	0.037	0.007	0.013	0.010	$1.04 \times 10^{-12}$	$1.08 \times 10^{-12}$	0.051	0.017
	Median	0.032	0.006	0.012	0.008	$8.94 \times 10^{-13}$	$9.24 \times 10^{-13}$	0.044	0.015
	Max	0.095	0.019	0.034	0.025	$2.66 \times 10^{-12}$	$2.75 \times 10^{-12}$	0.130	0.044
	Min	0.019	0.004	0.007	0.005	$5.31 \times 10^{-13}$	$5.49 \times 10^{-13}$	0.026	0.009
Pb	Mean	0.887	0.175	0.038	0.028	$2.46 \times 10^{-11}$	$2.55 \times 10^{-11}$	0.925	0.203
	Median	0.763	0.150	0.033	0.024	$2.11 \times 10^{-11}$	$2.20 \times 10^{-11}$	0.796	0.174
	Max	2.278 *	0.449	0.098	0.072	$6.32 \times 10^{-11}$	$6.57 \times 10^{-11}$	2.376 *	0.521
	Min	0.434	0.086	0.019	0.014	$1.20 \times 10^{-11}$	$1.25 \times 10^{-11}$	0.453	0.099
HI-total (Children)				HI-total (Elderly)					
Mean	Median	Max	Min	Mean	Median	Max	Min		
1.42	1.19	3.10	0.654	0.374	0.321	0.892	0.218		

Note: \* = risk exists.

In relation to the non-cancer risk assessment as a whole for the HMs considered (HI-total; Figure 8), it could be observed that the Pb contained in the RDS from areas with high ADT (>13,3000 veh./day) generated the highest risks for both children (HI-total = 3.10) and the elderly (HI-total = 0.892) (Table 4). Although, for the elderly population, the HI-total value was close to the recommended limit (HI ≤ 1.0). On average, HI for Pb represented in the child population about 75% of HI-total, followed by HI-Cr (19%), HI-Cu (4%), and HI-Ni (2%). It was reported that one of the main sources of Pb in children’s blood was the ingestion of contaminated soil and sediments, and that was a recurrent problem in industrialized cities [79]. In contrast to the results obtained using the Igeo index for Cr, where its concentrations in the RDS were close to the background values of urban soils (see Table 1 and Figure 3), the findings showed that this HM had an elevated risk on human health due to its high toxicity (HI). The evaluation of this HM in the RDS should raise further concern because there are several studies that have reached similar findings regarding elevated risk from Cr in road environments with elevated ADTs [5].

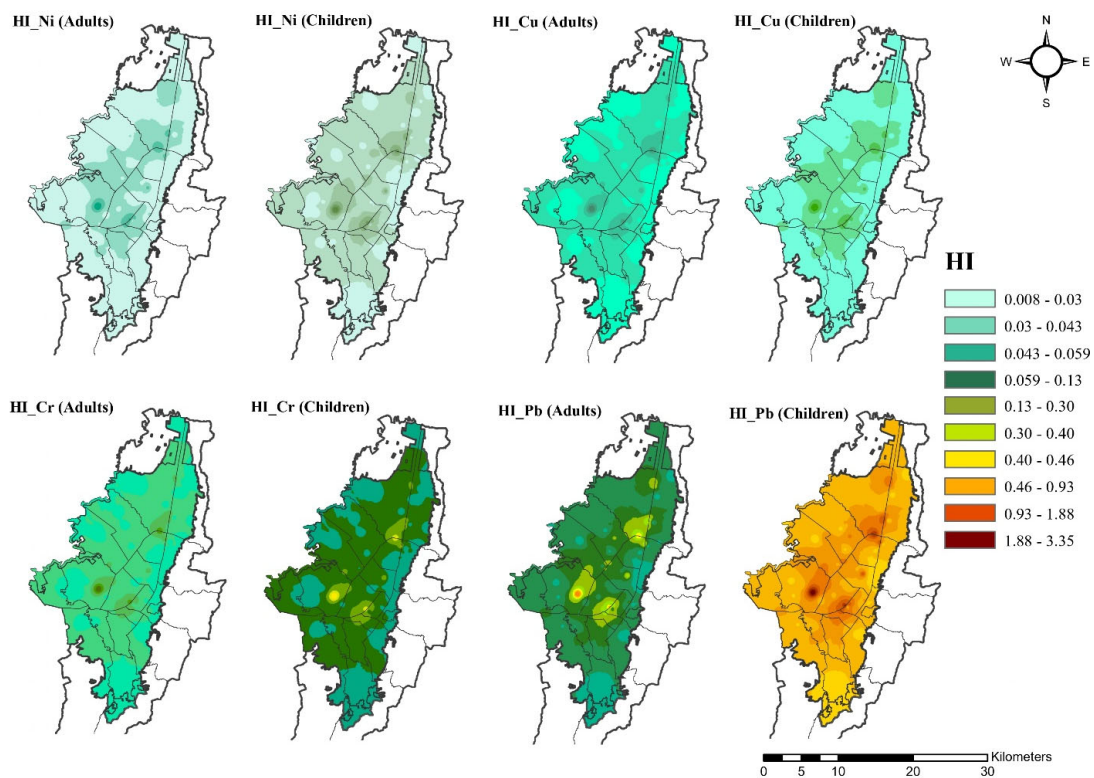


Figure 7. Spatial distribution of the HI index by HMs in children and elderly (Ni, Cr, Cu, and Pb).

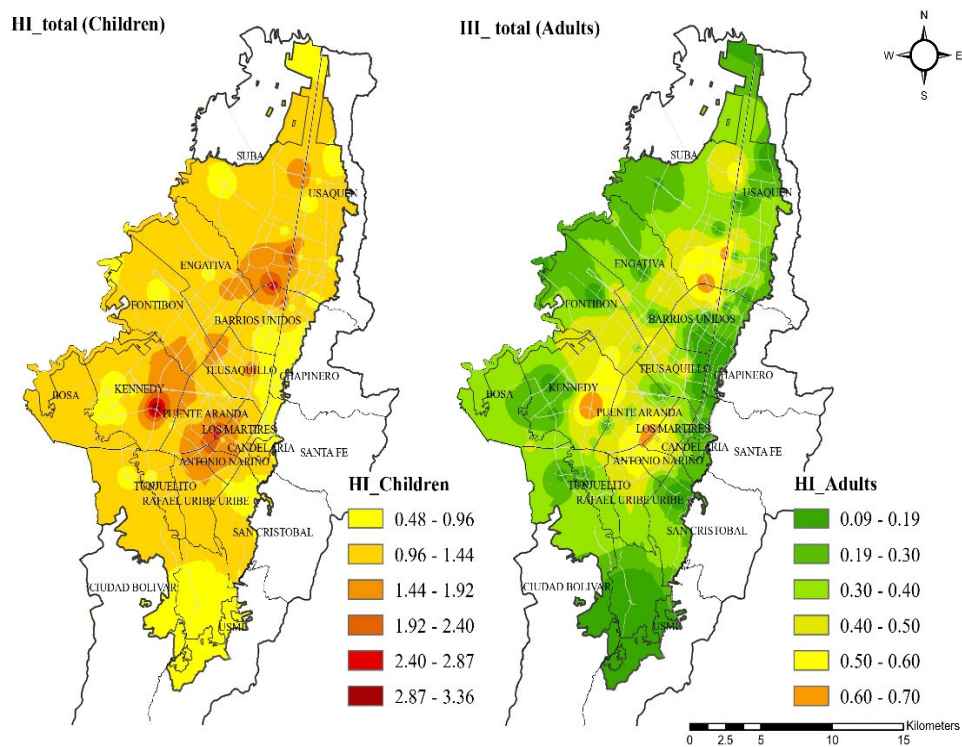


Figure 8. Spatial distribution of the HI-total index in children and elderly (Ni, Cr, Cu, and Pb).

In this study, we developed linear regression models between ADT and the HI index for each HM and the set of HMs considered (ingestion + contact + inhalation). That is, we normalized HM concentrations under the valuation scales established by this index. This normalization allowed a better fit of the linear regression models to be obtained between

ADT and the HI index ( $R^2 > 0.921$ ) compared to the models developed between ADT and HMs concentrations ( $R^2 > 0.322$ ). The linear regression models developed were as follows:  $HI_{Pb} = 2 \times 10^{-5} \times ADT + 0.334$  ( $R^2 = 0.971$ ),  $HI_{Cr} = 3 \times 10^{-6} \times ADT + 0.180$  ( $R^2 = 0.919$ ),  $HI_{Cu} = 6 \times 10^{-7} \times ADT + 0.0164$  ( $R^2 = 0.911$ ),  $HI_{Ni} = 1 \times 10^{-7} \times ADT + 0.008$  ( $R^2 = 0.901$ ), and  $HI_{total} = 2 \times 10^{-5} \times ADT + 0.436$  ( $R^2 = 0.992$ ). On the other hand, the results of the carcinogenic risk index (CRI) suggested that Cr was the HM of greatest attention. However, the concentrations of this HM in the RDS did not represent a carcinogenic risk ( $CRI < 1 \times 10^{-4}$ ). The maximum value in the CRI index ( $1.066 \times 10^{-6}$ ) was associated with the study road with the highest ADT (188,000 veh./day).

Based on the linear regression models developed to forecast HM concentrations, ADTs, and guidelines for human health protection, we proceeded to suggest ADT limits in the megacity under study. Guidelines on HM concentrations in urban residential land from Argentina and Catalonia (Spain) were considered as those with the greatest flexibility for the establishment of ADT limits. Furthermore, we considered the guidelines of Catalonia (Spain), Germany, and Canada as those with the highest requirement for the establishment of ADT limits. In this analysis, we considered the concentrations foretold at the 109 ADT monitoring stations and those observed at the nine direct monitoring stations. The linear regression models obtained were the following, with origin at zero:  $Pb = 0.0114 \times ADT$  ( $rs = 0.489$ ),  $Cu = 0.0052 \times ADT$  ( $rs = 0.538$ ), and  $Ni = 0.0006 \times ADT$  ( $rs = 0.687$ ). Table 5 shows the limiting ADTs (lower and upper) suggested for human health protection by HMs in the RDS. The results showed that 43.6% of the analyzed roads exceeded the upper ADT limit for Pb (43,860 veh./day; Figure 9), and 31.7% of the roads exceeded the upper ADT limit for Cu (59,615 veh./day). This suggested that Pb was the HM that, despite being removed from gasoline, continued to evidence the greatest relative importance to vehicular traffic and impact on human health. Lastly, we observed roads with values higher than 2.50 times in relation to the Pb limit concentration established by more flexible reference guidelines (Argentina).

**Table 5.** Suggested ADT limits for the protection of human health on urban residential land (Pb, Cu, and Ni).

Guideline	Argentina and Catalonia, Spain	Germany and Catalonia, Spain	Canada and Catalonia, Spain
	Pb	Cu	Ni
Lower limit (mg/kg)	500	310	470
Upper limit (mg/kg)	60	60	50
	Suggested ADT limits (veh./day)		
Upper ADT limit	43,860	59,615	783,300
Lower ADT limit	5263	11,538	83,300

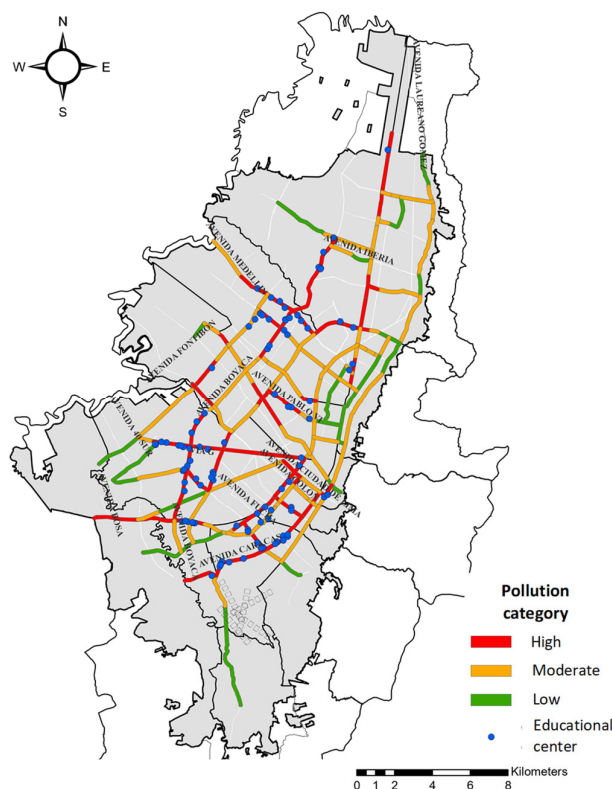


**Figure 9.** Categorization of the main roads in the study megacity according to the suggested ADT limit for Pb.

#### 4. Conclusions

The results of this study on the spatial variation in HM concentrations associated with the RDS from the ADT in a Latin American megacity allow us to draw the following conclusions.

1. The findings confirm that a size fraction  $< 250 \mu\text{m}$  is the most suitable to study risks of metallic enrichment (Igeo and IPI indices), ecological risks (ERI and CERI indices), and risks on human health (HI and CRI indices) due to the HMs associated with RDSs. This is under the hypothesis that ADT is the main indicator variable for the presence of HMs in the RDS  $< 250 \mu\text{m}$ . Thus, the best HM indicators of the above relationship are Ni, Cu, and Pb. These metallic elements can also serve as a basis for interventions aimed at reducing HM contamination levels in road transport systems.
2. From the indices used in this study, the following order of significance in the risk degree from HMs present in the RDS can be established: metallic enrichment (moderate to high)  $>$  ecological (moderate)  $>$  non-carcinogenic (non-significant)  $>$  carcinogenic (non-significant). However, the non-carcinogenic risk in the child population is significant and is mainly associated with the potential ingestion of RDSs.
3. The results show the following sequences in the risk degree for the main HMs considered in this study. Metal enrichment risk:  $\text{Pb} > \text{Cu} > \text{Ni} > \text{Cr}$ . Ecological risk:  $\text{Pb} > \text{Cu} > \text{Cr} > \text{Ni}$ . Non-carcinogenic risk:  $\text{Pb} > \text{Cr} > \text{Cu} > \text{Ni}$ . Carcinogenic risk:  $\text{Pb} > \text{Cr} > \text{Cu} > \text{Ni}$ . Thus, Pb is the HM of greatest attention, and Cr gains positions for its toxicity level during the evaluation of ecological, non-carcinogenic, and carcinogenic risks, respectively.
4. In the study megacity, we suggested the following ADT limits (lower and upper) for human health protection for Pb, Cu, and Ni in the RDS: 5263–43,860, 11,538–59,615, and 83,300–783,300 veh./day, respectively. Indeed, these limits in ADT tend to vary according to the type of risk analyzed (metallic enrichment, ecological, non-carcinogenic, and carcinogenic).

- The findings show that the linear regression models developed between ADT and each of the risk indices considered have a better fit ( $R^2 > 0.910$ ) compared to the linear regression models developed between ADT and HM concentrations ( $R^2 > 0.322$ ). Indeed, this improvement in the fit of the linear regression models developed is associated with the normalization of HM concentrations from the rating scales established by each of the risk indices considered. In addition, this also suggests the importance of considering other variables (e.g., land use and climate) when developing future studies on the relationship between traffic intensity, risk indices, and HM pollution.

**Author Contributions:** Conceptualization, A.V.G.-H. and C.A.Z.-M.; Methodology, A.V.G.-H., C.A.Z.-M. and H.A.R.-Q.; Software, A.V.G.-H.; Validation, A.V.G.-H. and C.A.Z.-M.; Formal analysis, A.V.G.-H., C.A.Z.-M. and H.A.R.-Q.; Investigation, A.V.G.-H. and C.A.Z.-M.; Resources, C.A.Z.-M.; Data curation, A.V.G.-H. and H.A.R.-Q.; Writing—original draft, A.V.G.-H.; Writing—review & editing, C.A.Z.-M. and H.A.R.-Q.; Visualization, A.V.G.-H., C.A.Z.-M. and H.A.R.-Q.; Supervision, C.A.Z.-M.; Project administration, C.A.Z.-M.; Funding acquisition, C.A.Z.-M. All authors have read and agreed to the published version of the manuscript.

**Funding:** This research received no external funding.

**Institutional Review Board Statement:** Not applicable.

**Informed Consent Statement:** Not applicable.

**Data Availability Statement:** Not applicable.

**Conflicts of Interest:** The authors declare no conflict of interest.

## References

- Wang, M.; Debbage, N. Urban Morphology and Traffic Congestion: Longitudinal Evidence from US Cities. *Comput. Environ. Urban Syst.* **2021**, *89*, 101676. [[CrossRef](#)]
- Bucsky, P.; Juhász, M. Long-Term Evidence on Induced Traffic: A Case Study on the Relationship between Road Traffic and Capacity of Budapest Bridges. *Transp. Res. Part A Policy Pract.* **2022**, *157*, 244–257. [[CrossRef](#)]
- Rybak, J.; Wróbel, M.; Krzyżyńska, R.; Rogula-Kozłowska, W.; Olszowski, T. Is Poland at Risk of Urban Road Dust? Comparison Studies on Mutagenicity of Dust. *Environ. Pollut.* **2022**, *314*, 120337. [[CrossRef](#)]
- Mitchell, G.; Oduyemi, K.; Akunna, J. Road Deposited Sediment: Implications for the Performance of Filter Drains Servicing Strategic Trunk Roads. *Water Sci. Technol.* **2019**, *80*, 747–761. [[CrossRef](#)]
- Aminiyani, M.M.; Baalousha, M.; Aminiyani, F.M. Evolution of Human Health Risk Based on EPA Modeling for Adults and Children and Pollution Level of Potentially Toxic Metals in Rafsanjan Road Dust: A Case Study in a Semi-Arid Region, Iran. *Environ. Sci. Pollut. Res.* **2018**, *25*, 19767–19778. [[CrossRef](#)]
- Sofia, D.; Lotrecchiano, N.; Trucillo, P.; Giuliano, A.; Terrone, L. Novel Air Pollution Measurement System Based on Ethereum Blockchain. *J. Sens. Actuator Netw.* **2020**, *9*, 49. [[CrossRef](#)]
- Zhao, H.; Li, X.; Wang, X.; Tian, D. Grain Size Distribution of Road-Deposited Sediment and Its Contribution to Heavy Metal Pollution in Urban Runoff in Beijing, China. *J. Hazard. Mater.* **2010**, *183*, 203–210. [[CrossRef](#)]
- Smichowski, P.; Gómez, D.R. An Overview of Natural and Anthropogenic Sources of Ultrafine Airborne Particles: Analytical Determination to Assess the Multielemental Profiles. *Appl. Spectrosc. Rev.* **2023**, *1*, 1–27. [[CrossRef](#)]
- Celo, V.; Yassine, M.M.; Dabek-Zlotorzynska, E. Insights into Elemental Composition and Sources of Fine and Coarse Particulate Matter in Dense Traffic Areas in Toronto and Vancouver, Canada. *Toxics* **2021**, *9*, 264. [[CrossRef](#)]
- Ali-Taleshi, M.S.; Squizzato, S.; Feiznia, S.; Carabali, G. From Dust to the Sources: The First Quantitative Assessment of the Relative Contributions of Emissions Sources to Elements (Toxic and Non-Toxic) in the Urban Roads of Tehran, Iran. *Microchem. J.* **2022**, *181*, 107817. [[CrossRef](#)]
- Al-Swadi, H.A.; Usman, A.R.A.; Al-Farraj, A.S.; Al-Wabel, M.I.; Ahmad, M.; Al-Faraj, A. Sources, Toxicity Potential, and Human Health Risk Assessment of Heavy Metals-Laden Soil and Dust of Urban and Suburban Areas as Affected by Industrial and Mining Activities. *Sci. Rep.* **2022**, *12*, 8972. [[CrossRef](#)]
- Dixit, R.; Wasiullah; Malaviya, D.; Pandiyan, K.; Singh, U.B.; Sahu, A.; Shukla, R.; Singh, B.P.; Rai, J.P.; Sharma, P.K.; et al. Bioremediation of Heavy Metals from Soil and Aquatic Environment: An Overview of Principles and Criteria of Fundamental Processes. *Sustainability* **2015**, *7*, 2189–2212. [[CrossRef](#)]
- Zaynab, M.; Al-Yahyai, R.; Ameen, A.; Sharif, Y.; Ali, L.; Fatima, M.; Khan, K.A.; Li, S. Health and Environmental Effects of Heavy Metals. *J. King Saud Univ.-Sci.* **2022**, *34*, 101653. [[CrossRef](#)]

14. Qu, J.; Li, Z.; Wu, Z.; Bi, F.; Wei, S.; Dong, M.; Hu, Q.; Wang, Y.; Yu, H.; Zhang, Y. Cyclodextrin-Functionalized Magnetic Alginate Microspheres for Synchronous Removal of Lead and Bisphenol a from Contaminated Soil. *Chem. Eng. J.* **2023**, *461*, 142079. [[CrossRef](#)]
15. Ermolin, M.S.; Fedotov, P.S.; Ivaneev, A.I.; Karandashev, V.K.; Fedyunina, N.N.; Burmistrov, A.A. A Contribution of Nanoscale Particles of Road-Deposited Sediments to the Pollution of Urban Runoff by Heavy Metals. *Chemosphere* **2018**, *210*, 65–75. [[CrossRef](#)]
16. Bezberdaya, L.A.; Kasimov, N.S.; Chernitsova, O.V.; Tkachenko, A.N.; Lychagin, M.Y. Heavy Metals and Metalloids in Soils, Road Dust, and Their PM10 Fractions in Sebastopol: Levels, Sources, and Pollution Risk. *Eurasian Soil Sci.* **2022**, *55*, 1871–1890. [[CrossRef](#)]
17. Lloyd, L.N.; Fitch, G.M.; Singh, T.S.; Smith, J.A. Characterization of Environmental Pollutants in Sediment Collected during Street Sweeping Operations to Evaluate Its Potential for Reuse. *J. Environ. Eng.* **2019**, *145*, 04018141. [[CrossRef](#)]
18. Kim, H.S.; Kim, K.-R.; Kim, W.-I.; Owens, G.; Kim, K.-H. Influence of Road Proximity on the Concentrations of Heavy Metals in Korean Urban Agricultural Soils and Crops. *Arch. Environ. Contam. Toxicol.* **2017**, *72*, 260–268. [[CrossRef](#)]
19. Gorka, R.; Kumar, R.; Yadav, S.; Verma, A. Health Implications, Distribution and Source Apportionment of Heavy Metals in Road Deposited Dust of Jammu City in Northern India. *Chemosphere* **2022**, *308*, 136475. [[CrossRef](#)]
20. Tang, Z.; Chai, M.; Cheng, J.; Jin, J.; Yang, Y.; Nie, Z.; Huang, Q.; Li, Y. Contamination and Health Risks of Heavy Metals in Street Dust from a Coal-Mining City in Eastern China. *Ecotoxicol. Environ. Saf.* **2017**, *138*, 83–91. [[CrossRef](#)]
21. Dietrich, M.; Krekeler, M.P.S.; Kousehlar, M.; Widom, E. Quantification of Pb Pollution Sources in Complex Urban Environments through a Multi-Source Isotope Mixing Model Based on Pb Isotopes in Lichens and Road Sediment. *Environ. Pollut.* **2021**, *288*, 117815. [[CrossRef](#)] [[PubMed](#)]
22. Botsou, F.; Sungur, A.; Kelepertzis, E.; Kypritidou, Z.; Daferera, O.; Massas, I.; Argyraki, A.; Skordas, K.; Soylak, M. Estimating Remobilization of Potentially Toxic Elements in Soil and Road Dust of an Industrialized Urban Environment. *Environ. Monit. Assess.* **2022**, *194*, 526. [[CrossRef](#)] [[PubMed](#)]
23. Ibañez-Del Rivero, C.; Fry, K.L.; Gillings, M.M.; Barlow, C.F.; Aelion, C.M.; Taylor, M.P. Sources, Pathways and Concentrations of Potentially Toxic Trace Metals in Home Environments. *Environ. Res.* **2023**, *220*, 115173. [[CrossRef](#)]
24. Shahab, A.; Zhang, H.; Ullah, H.; Rashid, A.; Rad, S.; Li, J.; Xiao, H. Pollution Characteristics and Toxicity of Potentially Toxic Elements in Road Dust of a Tourist City, Guilin, China: Ecological and Health Risk Assessment. *Environ. Pollut.* **2020**, *266*, 115419. [[CrossRef](#)] [[PubMed](#)]
25. Jeong, H.; Choi, J.Y.; Lee, J.; Lim, J.; Ra, K. Heavy Metal Pollution by Road-Deposited Sediments and Its Contribution to Total Suspended Solids in Rainfall Runoff from Intensive Industrial Areas. *Environ. Pollut.* **2020**, *265*, 115028. [[CrossRef](#)] [[PubMed](#)]
26. Böckin, D.; Tillman, A.-M. Environmental Assessment of Additive Manufacturing in the Automotive Industry. *J. Clean. Prod.* **2019**, *226*, 977–987. [[CrossRef](#)]
27. Adamiec, E.; Jarosz-Krzemińska, E.; Wieszala, R. Heavy Metals from Non-Exhaust Vehicle Emissions in Urban and Motorway Road Dusts. *Environ. Monit. Assess.* **2016**, *188*, 369. [[CrossRef](#)]
28. del Romero-Barreiro, M.P.; Pinilla-Castañeda, R.D.; Zafra-Mejía, C.A. Temporal Assessment of the Heavy Metals (Pb and Cu) Concentration Associated with the Road Sediment: Fontibón-Barrios Unidos (Bogotá D.C., Colombia). *Ing. Univ.* **2015**, *19*, 315–333. [[CrossRef](#)]
29. Men, C.; Liu, R.; Wang, Y.; Cao, L.; Jiao, L.; Li, L.; Shen, Z. A Four-Way Model (FEST) for Source Apportionment: Development, Verification, and Application. *J. Hazard. Mater.* **2022**, *426*, 128009. [[CrossRef](#)]
30. Lanzerstorfer, C. Heavy Metals in the Finest Size Fractions of Road-Deposited Sediments. *Environ. Pollut.* **2018**, *239*, 522–531. [[CrossRef](#)]
31. Williams, J.A.; Antoine, J. Evaluation of the Elemental Pollution Status of Jamaican Surface Sediments Using Enrichment Factor, Geoaccumulation Index, Ecological Risk and Potential Ecological Risk Index. *Mar. Pollut. Bull.* **2020**, *157*, 111288. [[CrossRef](#)] [[PubMed](#)]
32. Salman, S.A.; Zeid, S.A.M.; Seleem, E.-M.M.; Abdel-Hafiz, M.A. Soil Characterization and Heavy Metal Pollution Assessment in Orabi Farms, El Obour, Egypt. *Bull. Natl. Res. Cent.* **2019**, *43*, 42. [[CrossRef](#)]
33. Denny, M.; Baskaran, M.; Burdick, S.; Tummala, C.; Dittrich, T. Investigation of Pollutant Metals in Road Dust in a Post-Industrial City: Case Study from Detroit, Michigan. *Front. Environ. Sci.* **2022**, *10*, 1431. [[CrossRef](#)]
34. Duan, Z.; Wang, J.; Cai, X.; Wu, Y.; Xuan, B. Spatial Distribution and Human Health Risk Assessment of Heavy Metals in Campus Dust: A Case Study of the University Town of Huaxi. *Hum. Ecol. Risk Assess. Int. J.* **2020**, *26*, 986–999. [[CrossRef](#)]
35. Gupta, V.; Bisht, L.; Arya, A.K.; Singh, A.P.; Gautam, S. Spatially Resolved Distribution, Sources, Exposure Levels, and Health Risks of Heavy Metals in <63 Mm Size-Fractionated Road Dust from Lucknow City, North India. *Int. J. Environ. Res. Public Health* **2022**, *19*, 12898. [[CrossRef](#)]
36. Hanfi, M.Y.; Seleznev, A.A.; Yarmoshenko, I.V.; Malinovsky, G.; Konstantinova, E.Y.; Alsafi, K.G.; Sakr, A.K. Potentially Harmful Elements in Urban Surface Deposited Sediment of Ekaterinburg, Russia: Occurrence, Source Apportionment and Risk Assessment. *Chemosphere* **2022**, *307*, 135898. [[CrossRef](#)]
37. Zhu, H.; Liu, X.; Xu, C.; Zhang, L.; Chen, H.; Shi, F.; Li, Y.; Liu, Y.; Zhang, B. The Health Risk Assessment of Heavy Metals (HMs) in Road Dust Based on Monte Carlo Simulation and Bio-Toxicity: A Case Study in Zhengzhou, China. *Environ. Geochem. Health* **2021**, *43*, 5135–5156. [[CrossRef](#)]

38. Krupnova, T.G.; Rakova, O.V.; Gavrilkina, S.V.; Antoshkina, E.G.; Baranov, E.O.; Yakimova, O.N. Road Dust Trace Elements Contamination, Sources, Dispersed Composition, and Human Health Risk in Chelyabinsk, Russia. *Chemosphere* **2020**, *261*, 127799. [[CrossRef](#)]
39. Men, C.; Wang, Y.; Liu, R.; Wang, Q.; Miao, Y.; Jiao, L.; Shoaib, M.; Shen, Z. Temporal Variations of Levels and Sources of Health Risk Associated with Heavy Metals in Road Dust in Beijing from May 2016 to April 2018. *Chemosphere* **2021**, *270*, 129434. [[CrossRef](#)] [[PubMed](#)]
40. East, J.; Montealegre, J.S.; Pachon, J.E.; Garcia-Menendez, F. Air Quality Modeling to Inform Pollution Mitigation Strategies in a Latin American Megacity. *Sci. Total Environ.* **2021**, *776*, 145894. [[CrossRef](#)] [[PubMed](#)]
41. Sierra-Porta, D.; Solano-Correa, Y.T.; Tarazona-Alvarado, M.; de Villavicencio, L.A.N. Linking PM10 and PM2.5 Pollution Concentration through Tree Coverage in Urban Areas. *CLEAN—Soil Air Water* **2023**, *51*, 2200222. [[CrossRef](#)]
42. Bustamante-Zapata, A.M.; Zafra-Mejía, C.A.; Rondón-Quintana, H.A. Influence of Vegetation on Outdoor Thermal Comfort in a High-Altitude Tropical Megacity: Climate Change and Variability Scenarios. *Buildings* **2022**, *12*, 520. [[CrossRef](#)]
43. Vanegas, S.; Trejos, E.M.; Aristizábal, B.H.; Pereira, G.M.; Hernández, J.M.; Murillo, J.H.; Ramírez, O.; Amato, F.; Silva, L.F.O.; Rojas, N.Y.; et al. Spatial Distribution and Chemical Composition of Road Dust in Two High-Altitude Latin American Cities. *Atmosphere* **2021**, *12*, 1109. [[CrossRef](#)]
44. Cuéllar-Álvarez, Y.; Guevara-Luna, M.A.; Belalcázar-Cerón, L.C.; Clappier, A. Well-to-Wheels Emission Inventory for the Passenger Vehicles of Bogotá, Colombia. *Int. J. Environ. Sci. Technol.* **2023**, *1*, 4805. [[CrossRef](#)]
45. Zafra, C.; Suárez, J.; Pachon, J.E. Public Health Considerations for PM10 in a High-Pollution Megacity: Influences of Atmospheric Condition and Land Coverage. *Atmosphere* **2021**, *12*, 118. [[CrossRef](#)]
46. Secretaría Distrital de Movilidad de Bogotá Datos Abiertos Secretaría Distrital de Movilidad. Available online: <https://datos-abiertos-sdm-movilidadbogota.hub.arcgis.com/search,%20accessed%20on%20January%2030,%202019> (accessed on 13 May 2023).
47. INVIAS Serie Histórica de Tránsito Promedio Diario Actualizada TPD 2018 Publicacion. Available online: <https://www.invias.gov.co/index.php/archivo-y-documentos/documentos-tecnicos/6609-serie-historica-de-transito-promedio-diario-actualizada-tpd-2016-publicacion> (accessed on 13 May 2023).
48. Nasrollahi, H.; Ahmadi, F.; Ebadollahi, M.; Najafi Nobar, S.; Amidpour, M. The Greenhouse Technology in Different Climate Conditions: A Comprehensive Energy-Saving Analysis. *Sustain. Energy Technol. Assess.* **2021**, *47*, 101455. [[CrossRef](#)]
49. dos Santos, P.R.S.; Fernandes, G.J.T.; Moraes, E.P.; Moreira, L.F.F. Tropical Climate Effect on the Toxic Heavy Metal Pollutant Course of Road-Deposited Sediments. *Environ. Pollut.* **2019**, *251*, 766–772. [[CrossRef](#)]
50. Pal, S.K.; Roy, R. Evaluating Heavy Metals Emission' Pattern on Road Influenced by Urban Road Layout. *Transp. Res. Interdiscip. Perspect.* **2021**, *10*, 100362. [[CrossRef](#)]
51. Choi, J.Y.; Jeong, H.; Choi, K.-Y.; Hong, G.H.; Yang, D.B.; Kim, K.; Ra, K. Source Identification and Implications of Heavy Metals in Urban Roads for the Coastal Pollution in a Beach Town, Busan, Korea. *Mar. Pollut. Bull.* **2020**, *161*, 111724. [[CrossRef](#)]
52. Gao, S.; Wang, X.; Li, H.; Kong, Y.; Chen, J.; Chen, Z. Heavy Metals in Road-Deposited Sediment and Runoff in Urban and Intercity Expressways. *Transp. Saf. Environ.* **2022**, *4*, tdb030. [[CrossRef](#)]
53. Baum, P.; Kuch, B.; Dittmer, U. Adsorption of Metals to Particles in Urban Stormwater Runoff—Does Size Really Matter? *Water* **2021**, *13*, 309. [[CrossRef](#)]
54. ISO SIST ISO 11047:1999; Soil Quality—Determination of Cadmium, Chromium, Cobalt, Copper, Lead, Manganese, Nickel and Zinc—Flame and Electrothermal Atomic Absorption Spectrometric Methods. International Organization for Standardization: Geneva, Switzerland, 1999. Available online: <https://standards.iteh.ai/catalog/standards/sist/6e5c2955-71f9-48de-be0b-58c161f04894/sist-iso-11047-1999> (accessed on 13 May 2023).
55. ISO 11466:1995; Soil Quality—Extraction of Trace Elements Soluble in Aqua Regia. American National Standards Institute: Geneva, Switzerland, 2007.
56. Zafra, C.; Temprano, J.; Tejero, I. The Physical Factors Affecting Heavy Metals Accumulated in the Sediment Deposited on Road Surfaces in Dry Weather: A Review. *Urban Water J.* **2017**, *14*, 639–649. [[CrossRef](#)]
57. Ma, X.; Hua, M.Z.; Ji, C.; Zhang, J.; Shi, R.; Xiao, Y.; Liu, X.; He, X.; Zheng, W.; Lu, X. Rapid Screening and Quantification of Heavy Metals in Traditional Chinese Herbal Medicines Using Monochromatic Excitation Energy Dispersive X-ray Fluorescence Spectrometry. *Analyst* **2022**, *147*, 3628–3633. [[CrossRef](#)] [[PubMed](#)]
58. Doustmohammadi, M.; Anderson, M. A Bayesian Regression Model for Estimating Average Daily Traffic Volumes for Low Volume Roadways. *Int. J. Stat. Probab.* **2018**, *8*, 143. [[CrossRef](#)]
59. Trujillo-González, J.M.; Torres-Mora, M.A.; Jiménez-Ballesta, R.; Zhang, J. Land-Use-Dependent Spatial Variation and Exposure Risk of Heavy Metals in Road-Deposited Sediment in Villavicencio, Colombia. *Environ. Geochem. Health* **2019**, *41*, 667–679. [[CrossRef](#)] [[PubMed](#)]
60. Krivokapić, M. Study on the Evaluation of (Heavy) Metals in Water and Sediment of Skadar Lake (Montenegro), with BCF Assessment and Translocation Ability (TA) by Trapa Natans and a Review of SDGs. *Water* **2021**, *13*, 876. [[CrossRef](#)]
61. Mamat, Z.; Haximu, S.; Zhang, Z.Y.; Aji, R. An Ecological Risk Assessment of Heavy Metal Contamination in the Surface Sediments of Bosten Lake, Northwest China. *Environ. Sci. Pollut. Res.* **2016**, *23*, 7255–7265. [[CrossRef](#)]
62. Tang, R.; Ma, K.; Zhang, Y.; Mao, Q. The Spatial Characteristics and Pollution Levels of Metals in Urban Street Dust of Beijing, China. *Appl. Geochem.* **2013**, *35*, 88–98. [[CrossRef](#)]

63. Kumar, D.; Rajasegarar, S.; Palaniswami, M. Geospatial Estimation-Based Auto Drift Correction in Wireless Sensor Networks. *ACM Trans. Sen. Netw.* **2015**, *11*, 1–39. [[CrossRef](#)]
64. Li, F.; Zhang, J.; Huang, J.; Huang, D.; Yang, J.; Song, Y.; Zeng, G. Heavy Metals in Road Dust from Xiandao District, Changsha City, China: Characteristics, Health Risk Assessment, and Integrated Source Identification. *Environ. Sci. Pollut. Res.* **2016**, *23*, 13100–13113. [[CrossRef](#)]
65. IDECA. Infraestructura de Datos Espaciales de Bogotá. Available online: <https://ideca.gov.co> (accessed on 13 May 2023).
66. Pant, P.; Harrison, R.M. Estimation of the Contribution of Road Traffic Emissions to Particulate Matter Concentrations from Field Measurements: A Review. *Atmos. Environ.* **2013**, *77*, 78–97. [[CrossRef](#)]
67. Baptista Neto, J.A.; Rangel, C.M.A.; Da Fonseca, E.M.; Do Nascimento, M.T.L.; De Oliveira Santos, A.D.; Rodrigues, B.C.B.; De Melo, G.V. Concentrations and Physicochemical Speciation of Heavy Metals in Urban Runoff Sediment from São Gonçalo—Rio de Janeiro/Brazil. *Environ. Earth Sci.* **2016**, *75*, 1209. [[CrossRef](#)]
68. Gunawardena, J.; Ziyath, A.M.; Egodawatta, P.; Ayoko, G.A.; Goonetilleke, A. Mathematical Relationships for Metal Build-up on Urban Road Surfaces Based on Traffic and Land Use Characteristics. *Chemosphere* **2014**, *99*, 267–271. [[CrossRef](#)] [[PubMed](#)]
69. Sager, M.; Chon, H.-T.; Marton, L. Spatial Variation of Contaminant Elements of Roadside Dust Samples from Budapest (Hungary) and Seoul (Republic of Korea) Including Pt, Pd and Ir. *Environ. Geochem. Health* **2015**, *37*, 181–193. [[CrossRef](#)] [[PubMed](#)]
70. Galatioto, F.; Masey, N.; Murrells, T.; Hamilton, S.; Pommier, M. Review of Road Dust Resuspension Modelling Approaches and Comparisons Analysis for a UK Case Study. *Atmosphere* **2022**, *13*, 1403. [[CrossRef](#)]
71. Apul, D.S.; Miller, E.; Jain, V. Road-Runoff Metal Concentrations in Toledo, Ohio, and Their Relation to Average Daily Traffic and Age of Pavement Overlay. *Water Sci. Technol.* **2010**, *61*, 1723–1731. [[CrossRef](#)]
72. Alekseenko, V.; Alekseenko, A. The Abundances of Chemical Elements in Urban Soils. *J. Geochem. Explor.* **2014**, *147*, 245–249. [[CrossRef](#)]
73. Wei, X.; Gao, B.; Wang, P.; Zhou, H.; Lu, J. Pollution Characteristics and Health Risk Assessment of Heavy Metals in Street Dusts from Different Functional Areas in Beijing, China. *Ecotoxicol. Environ. Saf.* **2015**, *112*, 186–192. [[CrossRef](#)]
74. Gope, M.; Masto, R.E.; George, J.; Hoque, R.R.; Balachandran, S. Bioavailability and Health Risk of Some Potentially Toxic Elements (Cd, Cu, Pb and Zn) in Street Dust of Asansol, India. *Ecotoxicol. Environ. Saf.* **2017**, *138*, 231–241. [[CrossRef](#)]
75. Dehghani, S.; Moore, F.; Keshavarzi, B.; Hale, B.A. Health Risk Implications of Potentially Toxic Metals in Street Dust and Surface Soil of Tehran, Iran. *Ecotoxicol. Environ. Saf.* **2017**, *136*, 92–103. [[CrossRef](#)]
76. Abdel-Latif, N.M.; Saleh, I.A. Heavy Metals Contamination in Roadside Dust along Major Roads and Correlation with Urbanization Activities in Cairo, Egypt. *J. Am. Sci.* **2012**, *8*, 379–389.
77. Xu, D.-M.; Zhang, J.-Q.; Yan, B.; Liu, H.; Zhang, L.-L.; Zhan, C.-L.; Zhang, L.; Zhong, P. Contamination Characteristics and Potential Environmental Implications of Heavy Metals in Road Dusts in Typical Industrial and Agricultural Cities, Southeastern Hubei Province, Central China. *Environ. Sci. Pollut. Res.* **2018**, *25*, 36223–36238. [[CrossRef](#)] [[PubMed](#)]
78. Borai, E.H.; El-Sofany, E.A.; Abdel-Halim, A.S.; Soliman, A.A. Speciation of Hexavalent Chromium in Atmospheric Particulate Samples by Selective Extraction and Ion Chromatographic Determination. *TrAC Trends Anal. Chem.* **2002**, *21*, 741–745. [[CrossRef](#)]
79. Du, Y.; Gao, B.; Zhou, H.; Ju, X.; Hao, H.; Yin, S. Health Risk Assessment of Heavy Metals in Road Dusts in Urban Parks of Beijing, China. *Procedia Environ. Sci.* **2013**, *18*, 299–309. [[CrossRef](#)]

**Disclaimer/Publisher’s Note:** The statements, opinions and data contained in all publications are solely those of the individual author(s) and contributor(s) and not of MDPI and/or the editor(s). MDPI and/or the editor(s) disclaim responsibility for any injury to people or property resulting from any ideas, methods, instructions or products referred to in the content.